

Genetic isolation of transport signals directing cell surface expression

Sojin Shikano¹, Brian Coblitz¹, Haiyan Sun¹ and Min Li^{1,2}

Membrane proteins represent approximately 30% of the proteome in both prokaryotes and eukaryotes¹. The spatial localization of membrane-bound proteins is often determined by specific sequence motifs² that may be regulated in response to physiological changes, such as protein interactions³ and receptor signalling⁴. Identification of signalling motifs is therefore important for understanding membrane protein expression, function and transport mechanisms. We report a genetic isolation of novel motifs that confer surface expression. Further characterization showed that SWTY, one class of these isolated motifs with homology to previously reported forward transport motifs⁵, has the ability to both override the RKR endoplasmic reticulum localization signal and potentiate steady-state surface expression. The genetically isolated SWTY motif is functionally interchangeable with a known motif in cardiac potassium channels and an identified motif in an HIV coreceptor, and operates by recruiting 14-3-3 proteins. This study expands the repertoire of and enables a screening method for membrane trafficking signals.

We hypothesize that within a random pool of peptide sequences, each would possess a certain degree of surface expression potential (SEP). In a diversity space of random amino-acid sequences, one predicts that a large majority of sequences would have no effect on membrane protein localization. Hence a plot of number of sequences against SEP value would show a large number of sequences clustered near zero (Fig. 1a). This hypothesis further predicts that the ability of a protein to express on the cell surface would be the net of these two opposing forces, with negative or positive SEP values, which are subject to other regulatory activities including, for example, accessibility⁶, zoning of a signal motif⁷ and post-translational modification⁵. Neither DXE^{8,9} nor FCYENE¹⁰ overrides RKR³ or KKXX¹¹ endoplasmic reticulum (ER) localization motifs for surface expression, suggesting that they are recessive. We sought motifs that might override RKR or KKXX, because known forward signals such as DXE and FCYENE do not.

We developed a genetic screen to identify sequences to override an ER localization signal and to potentiate steady-state surface expression

using the Kir2.1 inward rectifier potassium channel as a reporter protein, which is capable of complementing the yeast mutant SGY1528 with double knockout of *TRK1* and *TRK2* genes to grow in normal potassium media (~4 mM)¹². Fusion of Kir2.1 with an ER localization signal such as the RKR motif leads to effective intracellular localization in mammalian cells⁷, and abolishes its ability to complement the growth of SGY1528 (Fig. 1b), consistent with the notion that RKR is *cis*-dominant over FCYENE, endogenous to Kir2.1. Furthermore, a mutant of RKR to RAA regained its ability to complement (Fig. 1b). Using this reporter system, we constructed a random peptide library carboxy-terminal to the RKR motif to screen for dominant signals capable of transporting the reporter to the cell surface¹³. The initial screen of ~2 × 10⁶ recombinants has identified 206 clones. Upon confirmation by retransformation, 64 distinct sequences were isolated (Fig. 1d).

To identify those functional in mammalian cells, the sequences were transferred to a mammalian cell expression vector and individually expressed via transient transfection in HEK293 cells. The surface expression of an otherwise ER-localized HA-tagged Kir2.1-RKR protein was evaluated by anti-HA antibody and quantified with flow cytometry. On the basis of their effectiveness in conferring surface expression of Kir2.1-RKR, these sequences may be divided into three groups (Fig. 1d, e). Group 1 shows essentially no detectable surface expression, similar to that of the reporter fusion of Kir2.1-RKR. This group may represent those motifs possessing activity specific in yeast, or a different mechanism to rescue the yeast growth. Group 2 sequences are those capable of directing surface expression at a level similar to that of the wild-type Kir2.1. Group 3 comprises motifs conferring surface expression levels higher than that of wild type. This represents a gain of function by potentiating the surface expression of the channel protein.

Both electrophysiological recording and a rubidium flux assay found that Kir2.1-RKR-SWTY (clone #4) showed normal function with no detectable difference in voltage activation or other biophysical properties from wild-type Kir2.1 channels (data not shown). The RGRSWTY (#4) motif (termed SWTY) was selected for further analyses because of its potency in potentiating surface expression. To test whether the SWTY effect is RKR-dependent, we compared the expression of Kir2.1-RKR-SWTY and Kir2.1-RAA-SWTY. The flow cytometry data indicate that

¹Department of Neuroscience and High Throughput Biology Center, Johns Hopkins University School of Medicine, 733 North Broadway, Baltimore, MD 21205, USA.

²Correspondence should be addressed to M.L. (e-mail: minli@jhmi.edu)

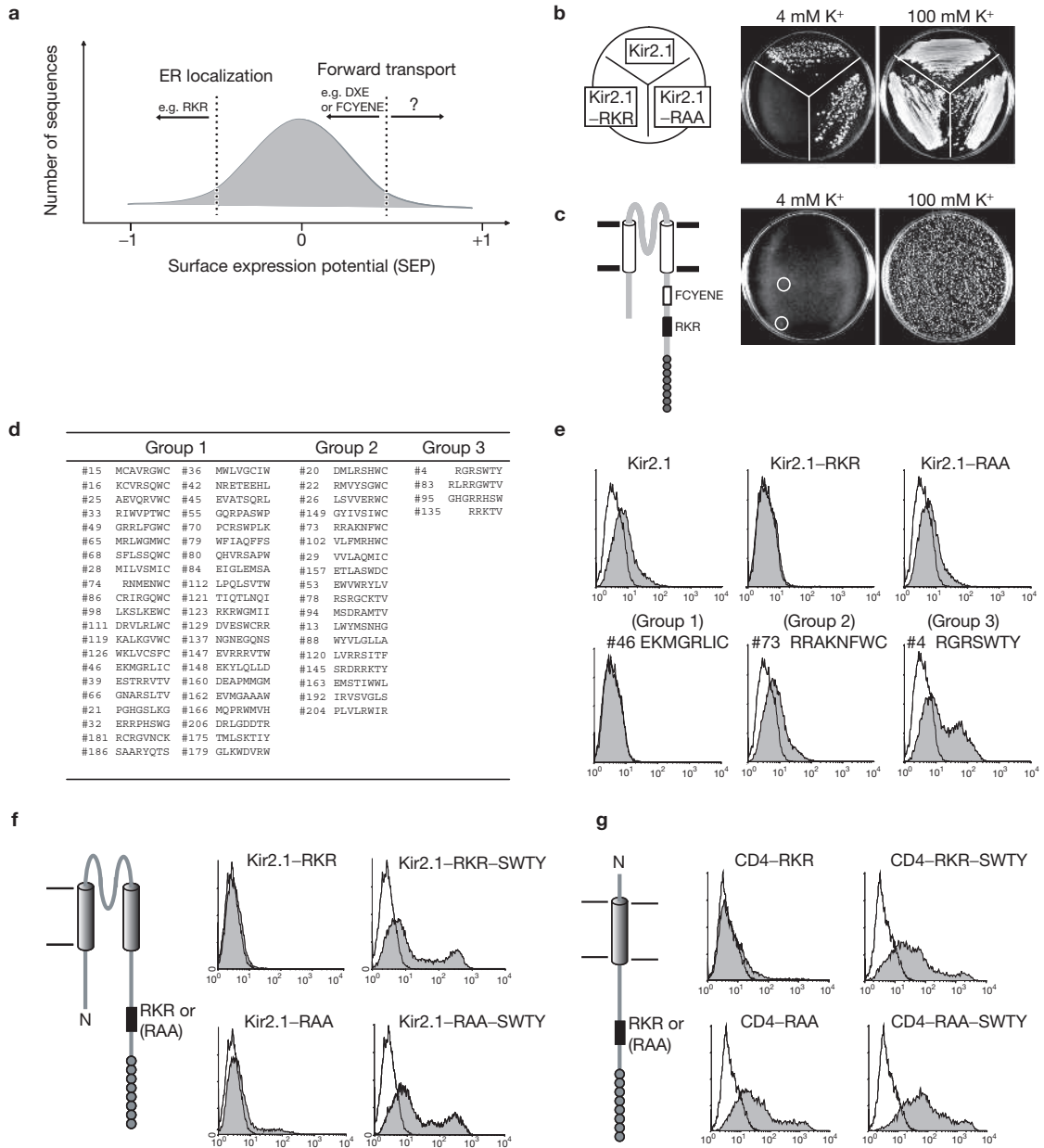


Figure 1 Design of a genetic screen system. **(a)** Hypothesis of cell surface expression potential (SEP). A schematic plot shows the number of sequences from a random peptide library (vertical axis) as a function of ability to confer either surface expression or intracellular localization (horizontal axis). The shape and symmetry of the graph need not be as shown. Hypothetical thresholds of SEP values for ER localization signals and forward transport signals are shown by dashed lines. **(b)** Yeast growth test of Kir2.1 channel with different fusion peptides. **(c)** An example of library selection. Left: a schematic diagram of the Kir2.1 reporter. Right: growth comparison of ~10,000 library transformants in indicated

potassium media. Colonies grown in a selection plate are circled. **(d)** Deduced amino-acid sequences from an X8 random peptide screen. Sequences are grouped according to their ability to confer surface expression of Kir2.1-RKR. **(e)** Flow cytometry analyses of HA-tagged Kir2.1 channel in HEK293 cells. Grey areas are staining signals. Mock-transfected cells stained with primary and secondary antibodies served as background (unfilled areas). The transfected constructs are as indicated. **(f, g)** Left panels: schematic diagrams of Kir2.1-RKR-SWTY **(f)** or CD4-RKR-SWTY **(g)**. Right panels: flow cytometry analyses to compare surface expression of SWTY-tagged Kir2.1 **(f)** or CD4 **(g)** with RKR or RAA motifs.

both constructs, regardless of RKR or RAA, showed comparable expression, higher than that of wild type (Fig. 1f; right panels). These results support that RGRSWTY conferred a gain of function.

Most potassium channels are tetramers¹⁴. To evaluate whether the SWTY motif is reporter-specific, we selected CD4, a monomeric type I membrane protein with robust surface expression. A fusion of CD4 with the RKR motif markedly reduced the surface expression to a background

level. Similar to Kir2.1, mutation of RKR to RAA restored the surface expression. In the presence of the SWTY motif, CD4 surface expression no longer showed any effect from RKR, indicating that SWTY was again effective and overriding the effect of RKR (Fig. 1g). The surface expressions in CD4-RKR-SWTY or CD4-RAA-SWTY were slightly higher than that of CD4-RAA but less pronounced compared with Kir2.1, presumably due to the already robust expression of CD4; although one

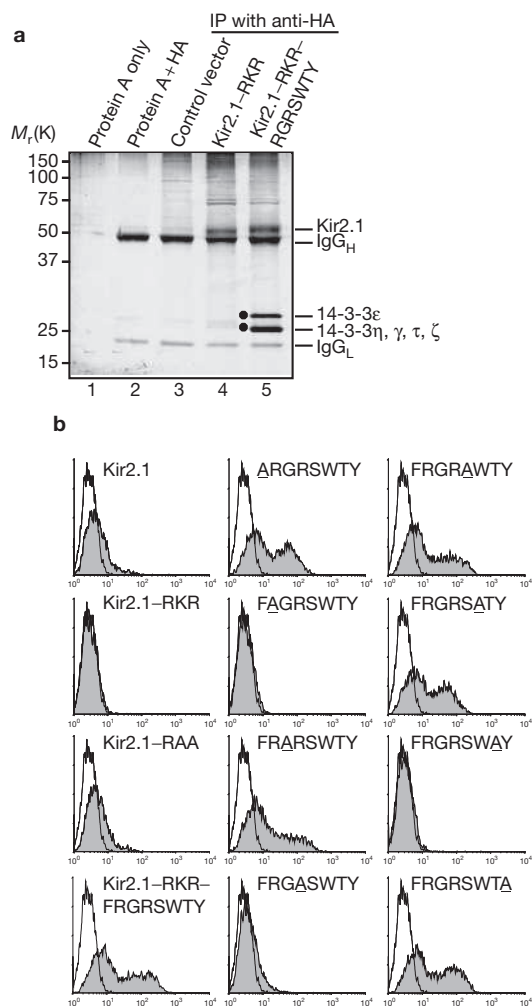
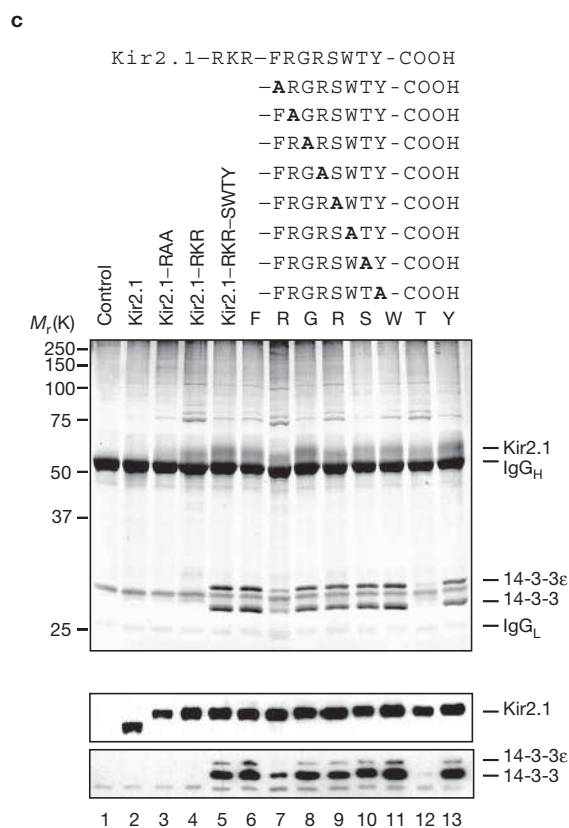


Figure 2 Interaction of the SWTY motif with 14-3-3 proteins. **(a)** Image of a silver-stained gel of proteins isolated by immunoprecipitation. Lane 1, Protein A alone; lane 2, Protein A plus anti-HA antibody; lanes 3–5, anti-HA precipitation from lysates of cells transfected with mock vector (lane 3), Kir2.1-RKR construct (lane 4) or Kir2.1-RKR-RGRSWTY construct (lane 5). The proteins confirmed by MALDI-TOF are identified on the right. **(b)** Histograms of flow cytometry analyses of HA-tagged

cannot rule out that the different oligomeric states of CD4 and Kir2.1 affect the extent of elevated surface expression. Together, the results demonstrate that the SWTY motif is effective in overriding RKR-mediated ER localization in two unrelated proteins.

The SWTY-elevated expression suggests that the motif may function by recruiting protein machinery that actively mediates the surface expression of membrane protein. To test this hypothesis, HEK293 cells were transfected with HA-tagged Kir2.1 constructs and the anti-HA immunoprecipitates of cell lysates were fractionated and visualized by silver stain (Fig. 2a). Two distinct bands with relative molecular masses of 30,000 (M_r 30K) and 28,000 (M_r 28K) were found specifically from Kir2.1-RKR-SWTY-transfected cells (Fig. 2a; lane 5). These polypeptides were determined by matrix-assisted laser desorption/ionisation-time of flight (MALDI-TOF) mass spectrometry to correspond to 14-3-3 isoforms¹⁵ with the higher relative molecular mass band being 14-3-3 ϵ , and the lower band being a mixture of at least four isoforms including γ , η , τ and ζ . The specific and direct interaction between Kir2.1-RKR-SWTY and 14-3-3 isoforms was



Kir2.1 using anti-HA antibody. Constructs for each transfection are as indicated. **(c)** Immunoprecipitation with anti-HA antibody. Lanes 1 to 5 are immunoprecipitates of transfected cell lysates from the indicated vectors. Lanes 6 to 13 are from alanine-substituted mutants. Top panel is an image of the silver-stained gel. 14-3-3 proteins are identified on the right. Middle and lower panels are immunoblots of the same material probed with anti-Kir2.1 antibody and anti-14-3-3 antibody, respectively.

further tested and confirmed using recombinantly expressed 14-3-3 isoforms in either mammalian cells or in purified forms (data not shown).

To be more definitive, the residues critical for 14-3-3 binding and surface expression were examined by alanine substitutions scanning the FRGRSWTY motif. Of the eight alanine mutants, FAGRSWTY and FRGRSWAY were most effective, completely abolishing surface expression (Fig. 2b). Thus, the -2 threonine and upstream arginine residues are critical for elevated surface expression. The ability to bind to 14-3-3 was shown by co-immunoprecipitation (Fig. 2c). The 14-3-3 species were only detectable in SWTY-transfected cells (Fig. 2c; lanes 1 to 5). The silver staining patterns of the alanine-scanning mutants showed differential 14-3-3 intensities correlating with the ability of mutants to bind to 14-3-3 isoforms. Specifically, both FAGRSWTY and FRGRSWAY showed a marked reduction of 14-3-3 binding (Fig. 2c; lanes 7 and 12). The reduction of 14-3-3 was further substantiated by immunoblotting against 14-3-3, which also showed a reduction (lane 7) and loss of signal (lane 12). These results substantiate the link between the 14-3-3 binding and surface expression.

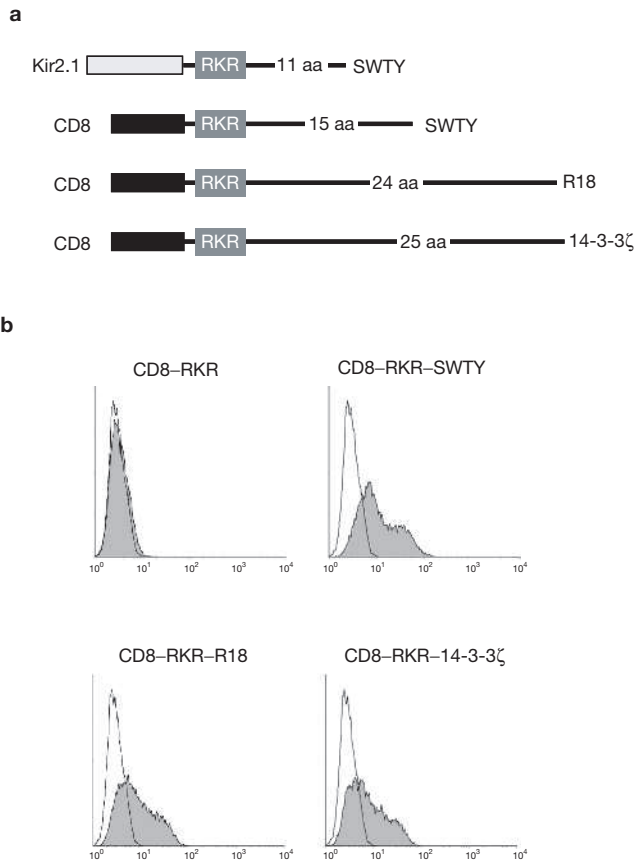


Figure 3 Overriding of RKR ER localization by SWTY, R18 and fused 14-3-3. **(a)** Schematic diagram of the indicated fusion constructs. The numbers of amino-acid residues (aa) separating RKR motif from 14-3-3 binding motifs (or the fused 14-3-3) are as indicated. **(b)** Histograms of flow cytometry analyses of the indicated constructs. Full-length protein expression of these constructs has been verified by immunoblots (data not shown).

To test whether the effects are 14-3-3-dependent and sensitive to sequence or the length of linker between RKR and 14-3-3, we constructed three CD8 fusion proteins (Fig. 3a). Compared with the Kir2.1-RKR-SWTY construct, which has an 11-residue linker, the linkers of the three constructs were progressively elongated to 16-, 24- and 25-amino-acid residues. In the CD8-RKR-R18 construct, the SWTY motif was replaced with the non-homologous R18 sequence (PHCVPRDLSWLDLEANMCLP), a 14-3-3-binding peptide that was identified from a non-phosphorylated random peptide library¹⁶. In the CD8-RKR-14-3-3 ζ construct, the SWTY motif was replaced with the entire coding sequence of human 14-3-3 ζ cDNA. Figure 3b shows that both R18 and 14-3-3 ζ are capable of overriding RKR, with effects comparable to that of SWTY. Hence, independent from the sequence of SWTY, either *trans*-recruitment of 14-3-3 by R18 or *cis*-fusion of 14-3-3 protein itself is sufficient to override RKR-mediated ER localization. However, these results could not formally exclude the possible interference of 14-3-3 with ER localization machinery.

The elevated surface expression after 14-3-3 binding could originate from one or multiple steps, including an increased rate of vesicular transport and a reduced rate of endocytosis. We performed functional recovery after a chemobleaching (FRAC) assay¹⁷, which revealed no detectable difference in the rate of forward transport (see Supplementary Information, Fig. S1). In contrast, the results of pulse-chase analyses

indicate prolongation of surface half-life by the SWTY motif (see Supplementary Information, Fig. S2).

The SWTY motif is different from the canonical 14-3-3-binding consensus: -RSXpSXP- and -RXXpSXP^{18,19}. Among 19 selected clones in Groups 2 and 3 (Fig. 1d), the six clones were found to interact with 14-3-3 (Fig. 4a). Despite their differences in length and surface expression levels (Fig. 4b), these six sequences possess clearly shared features including serine or threonine at the -2 position and positively charged residues upstream. To determine the potential preference in positioning at -2 for threonine or serine, we constructed and expressed a mutant of Kir2.1-RKR-SWTY, which has three additional alanines fused to the C terminus. Flow cytometry analyses revealed that adding AAA to the C terminus of SWTY abolished SWTY-mediated surface expression (Fig. 4c). To determine whether the phosphorylation of -2 threonine or serine has a role, an affinity precipitation experiment was performed using synthetic peptides corresponding to a control sequence (SISPDLSL), and three forms of the SWTY sequence: RGRSWTY, RGRSWpTY and RGRSWpTYAAA. The results indicate that only RGRSWpTY was capable of precipitating 14-3-3 (Fig. 4d; lane 4). Hence, phosphorylation at the -2 position of the SWTY motif is important for the 14-3-3 interaction. This supports the idea of a new mode (mode III) of the 14-3-3 binding²⁰.

To examine native proteins with SWTY-like sequences, we performed bioinformatics analyses to search for proteins with C termini that match the specific criteria. Fig. 5a summarizes the filtering criteria and more than 200 hits from different species representing membrane proteins of diverse functions including cytokine receptors, G-protein-coupled receptors (GPCRs), ion channels, transporters and membrane-associated cytosolic proteins. A list of the shown native sequences from different species was tested for overriding the RKR motif in CD8 for surface expression. The results indicate that for these proteins the ability to confer surface expression coincides with their ability to bind 14-3-3 proteins, indicative of the possession of functional similarity to the SWTY motif (Fig. 5b).

To test the activity of the SWTY-like sequence in the native context, we selected two markedly different proteins: KCNK3, a potassium channel, and GPR15, a G-protein-coupled receptor. KCNK3 is important for controlling membrane potential²¹. Earlier work showed that the C-terminal domain of KCNK3 has the ability to interact with 14-3-3, and such an interaction correlates with the ability of KCNK3 to express on the cell surface⁵. Because the ER localization signal of KCNK3 is located at the N-terminal domain, distant from the C-terminal 14-3-3-binding sequences, this evidence argues for the notion that 14-3-3 has a positive role in overriding ER signals to confer the forward transport. Another protein we chose is GPR15, a member of the GPCR superfamily and a coreceptor for HIV^{22,23}. These two proteins have SWTY-like sequences (Fig. 5b), and transient expression of wild-type KCNK3 or GPR15 in cultured HEK293 cells resulted in surface expression that was readily detected (Fig. 5c). Point mutations at the C terminus, KCNK3^{S410A} or GPR15^{S359A}, diminished surface expression as judged by both confocal imaging and flow cytometry (Fig. 5c). The robust surface expression of KCNK3 and GPR15 could be restored by replacing their C termini with RGRSWTY but not RGRSWAY motifs (Fig. 5d). The surface expression of mutants is directly correlated with the ability of binding 14-3-3 (Fig. 5e). These results show that the *de novo* isolated sequence, RGRSWTY, is mechanistically compatible with the two native

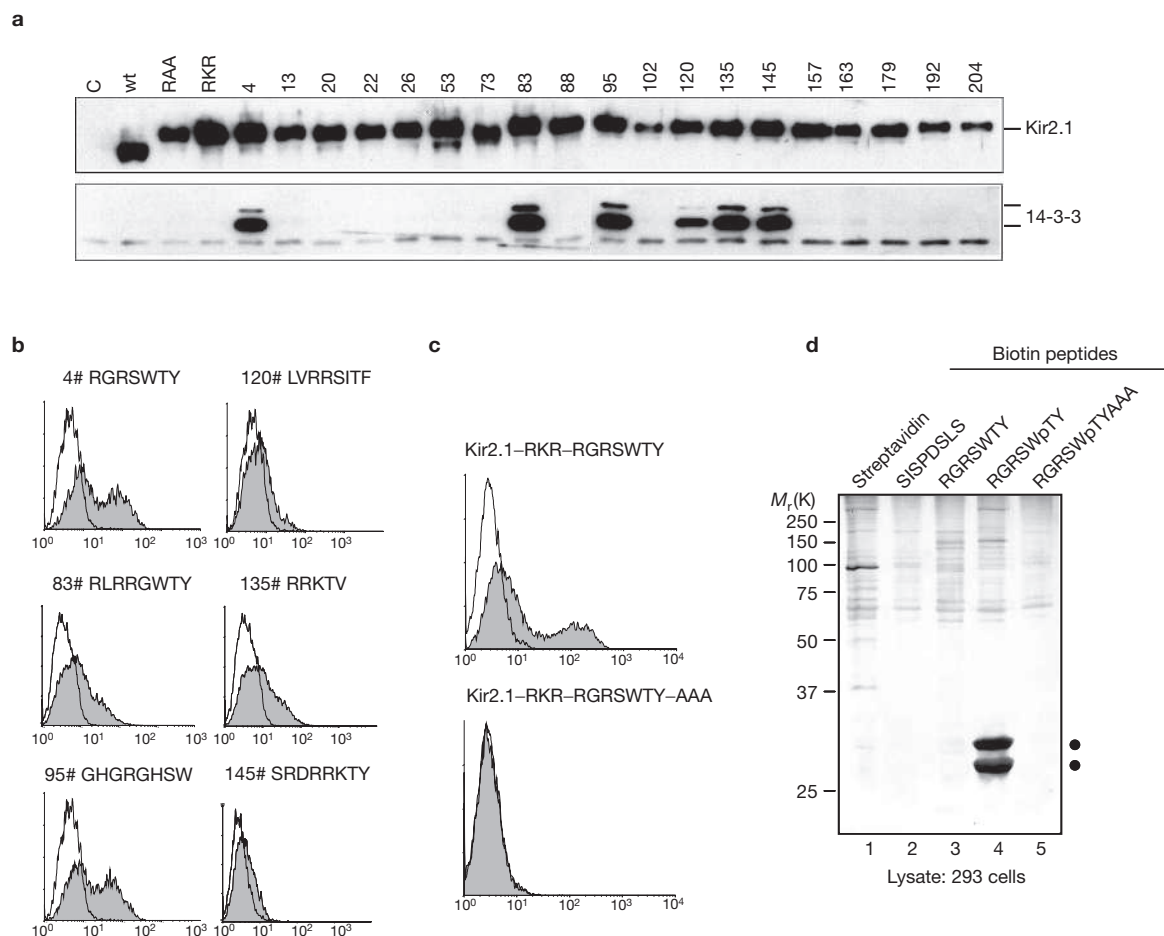


Figure 4 Phosphorylation-dependent interaction between 14-3-3 and SWTY-related motifs. **(a)** Anti-HA precipitated materials for indicated transfections were immunoblotted by anti-Kir2.1 antibody (upper panel) and by anti-14-3-3 antibody (lower panel). **(b)** Flow cytometry analyses of surface expression of Kir2.1 fusions with indicated 14-3-3-binding

clones. **(c)** Flow cytometry analyses of surface expression of Kir2.1-SWTY and Kir2.1-SWTY-AAA. **(d)** Affinity precipitation of 14-3-3 proteins from HEK293 cells by streptavidin-conjugated beads with bound biotin peptides (as indicated). The affinity-precipitated materials were visualized by silver stain.

C-terminal sequences of KCNK3 (LMKKRRSSV) and GPR15 (RRKRSVSL). Furthermore, these experiments, using two markedly different native proteins, provide direct evidence linking sequence to phosphorylation to 14-3-3 binding and then to surface expression.

Our findings suggest the existence of *cis*-dominant signal motifs that override an ER localization signal. Earlier reports suggest a role for 14-3-3 in receptor forward transport^{5,24}. The causal relationship of 14-3-3 binding and surface expression is established by both detailed mutagenesis studies of SWTY (Fig. 2) and by non-SWTY-mediated 14-3-3 recruitment including R18 peptide and the covalent fusion of 14-3-3 protein (Fig. 3). SWTY probably exemplifies a general theme that these types of motifs are functionally plastic by remaining silent unless a signal activates appropriate enzymatic and interaction machinery. *In vivo*, whether and under what physiological conditions recruitment of 14-3-3 proteins occurs could depend on a number of factors including both expression and activation of specific kinases or phosphatases, and sequence compatibility to 14-3-3 binding. These factors may vary according to organisms, cell types and physiological states. Because the ability to recruit 14-3-3 is sufficient to override RKR (Figs 2 and 3), the number of native proteins with SWTY-like signals listed in Fig. 5a is likely to be underestimated as it does not include canonical sequences known for 14-3-3 binding.

It is well known that 14-3-3 recognition is specifically coupled to the activation of a variety of kinases in signalling^{18,25}. The role of 14-3-3 in intracellular localization has been well appreciated²⁶. The activity of 14-3-3 in transport of membrane protein was implicated with curious phosphorylation-independent²⁴ and -dependent modes²⁷.

The identification of SWTY and related sequences indicates the existence of strong surface expression motifs. With regard to overriding ER localization activity, current evidence supports that a direct interaction between known ER export motifs and protein export machinery is involved in ER exit^{28,29}. SWTY and its related sequences appear to have no homology to well characterized ER export motifs, such as DXE⁸ and FCYENE¹⁰, consistent with the findings that neither is capable of overriding ER localization. The other identified sequence motifs reveal significant sequence divergence from SWTY (Fig. 1d), indicative of different mechanisms of action. Interestingly, 18 out of 64 sequences end with 'WC-COOH'. Examination of the yeast genome revealed a total of 10 open reading frames coding for WC termini³⁰; all are membrane proteins, nine of which are permeases responsible for removing toxic small molecules to yeast. The conservation of the WC motif among these otherwise diverse 18 sequences suggests a shared mechanism of action. Hence, the specific mechanistic details concerning SWTY and

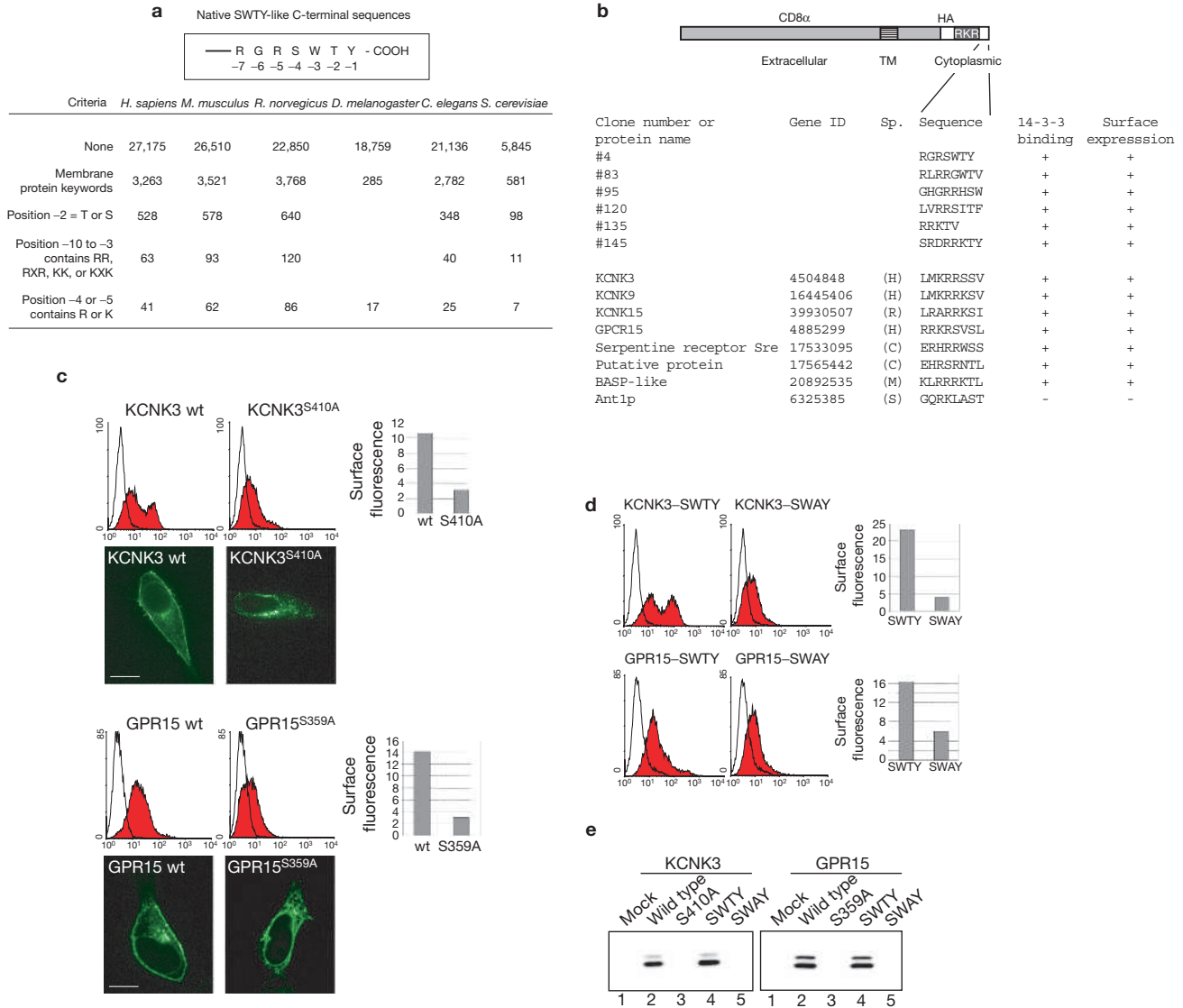


Figure 5 Native SWTY-like sequences. **(a)** Identification of native C-terminal sequences for similarity to RGRSWTY. The species and specific criteria used are listed on the left. The numbers of genes matching each sequentially filtered criterion are listed. Redundant splice variants of one gene are listed as one hit. **(b)** Schematic diagram of the CD8 construct, which includes an HA epitope, a RKR motif and fused SWTY or SWTY-like sequences. The sequences from either the random peptide library or from selected genes identified from a bioinformatics search are aligned and identified by clone number or protein name, gene ID and species. The ‘+’ or ‘-’ indicates their abilities to bind to 14-3-3 and to override RKR signals as determined by co-immunoprecipitation and flow cytometry analyses. **(c)** Histograms show flow

cytometry analyses for surface expression of HA-tagged KCNK3 and GPR15 with and without (wt) the mutation of serine to alanine at the C-terminal -2 position (upper panels). The bar graphs show the quantification of surface expression according to the mean fluorescence intensity after subtraction with that of mock-transfected cells. Sublocalization of indicated constructs in permeabilized cells was analysed by confocal microscopy. **(d)** Flow cytometry analyses for surface expression of KCNK3 and GPR15 with their C-terminal sequences (RRSSV or RRKRSVSL) replaced with RGRSWTY or RGRSWAY. **(e)** Co-immunoprecipitation of 14-3-3 with KCNK3 and GPR15. Total lysates from transfected cells as indicated were immunoprecipitated by anti-HA antibody, and the eluates were blotted with anti-14-3-3 antibody.

other sequences are an interesting topic for future investigation. Our recent evidence indicates that SWTY has a similar binding affinity to that of canonical 14-3-3 binding peptides and the -1 position is tolerant to substitution of other residues³¹.

The motifs reported here may be useful in establishing elevated surface expression for poorly expressed cell surface receptors. It is known that a given receptor or channel protein often contains multiple transport signals³². The overall localization behaviour may be modelled according to the SEP values of individual, different transport signals present in the receptor. The evidence reported here demonstrates that one motif could have a determining role in shifting the overall

SEP value. Plasticity of a motif in switching among silent, active and intermediate states, for example, by phosphorylation, could regulate surface expression of one or a group of membrane receptors, hence inducing changes in cell physiology. □

METHODS

Molecular biology. The yeast expression vector for mammalian Kir2.1 was generated by cloning mouse *Kir2.1* cDNA in pADNS vector at *Hind*III and *Not*I. The artificial *Pst*I site was inserted at the C terminus of Kir2.1 by replacing the last residue (I) with the *Pst*I sequence (LQ). The DNA fragment encoding the C-terminal 36 amino acids of mouse Kir6.2 (LLDALTLASSRGPLRKRSVAVAKA KPKFISISPLSL) was generated by annealing and extending the complementary

oligonucleotides with *Pst*I and *Not*I overhangs and then ligating to Kir2.1. DNA was also generated with a mutation of RKR to RAA to disrupt the ER localization signal. The *Sac*I site was engineered nine amino acids downstream of the RKR signal (this caused mutation of PK to EL) to replace SISPDSLs with the DNA fragments encoding an eight-amino-acid (X8) random peptide library³⁰. The X8 library DNA fragments were generated by annealing and extending the sense strand (5'-GAGCTCTTT(NNK)₈TAGGCGGCCGCTACATACA, where N indicates A, T, C, or G and K indicates either G or T) and antisense strand (5'-TGTATGTAGCGGCCGCTA) oligonucleotides that were synthesized to randomly encode eight amino acids preceded by phenylalanine with *Sac*I and *Not*I overhangs. *Escherichia coli* were transformed with Kir2.1-RKR-X8 library plasmids by electroporation and plated at 10,000 colonies per plate to isolate the plasmids. The mammalian expression vectors were constructed by transferring the chimeric *Kir2.1* cDNAs to a pcDNA3.1(+) vector (Invitrogen, Carlsbad, CA) at *Hind*III and *Not*I. For detection of surface expression, the HA epitope (YPYDVPDYA) was inserted at position 117 of Kir2.1. This HA was reported to cause no obvious effect on channel properties³. A CD4-3HA vector encoding human CD₄ extracellular and transmembrane domains attached with three HA repeats was generated as described⁷. The 36-amino-acid sequence of Kir6.2 was cloned into the C terminus of CD4-3HA at *Bam*HI and *Eco*RI. CH8-HA vectors were constructed by replacing the CD4 sequence in CD4-3HA vectors with full-length human CD8 α fused with the HA sequence. A mutagenesis of the FRGRSWTY sequence in clone#4 was performed by annealing and extending complementary oligonucleotides that contained individual mutations. Native C-terminal X8 sequences were cloned into a CD8 vector. Rat KCNK3 was cloned by PCR into pcDNA3.1(+) at *Hind*III and *Not*I with the HA epitope inserted at position 213 of KCNK3. Human GPR15 was cloned by PCR into pCMV vector at *Sal*I and *Not*I with the HA epitope at the N terminus.

Yeast screening for surface Kir2.1-expressing clones. SGY1528 (MATa; ade2-1; can1-100; his3-11,15; leu2-3,112; trp1-1; ura3-1; trk1::HIS3; trk2::TRP1) does not grow on low-potassium media but can be rescued by heterologous expression of Kir2.1. Yeast were transformed with pADNS plasmids and grown on drop-out media without leucine, supplemented with 100 mM KCl. Transformants were then plated on 4 mM KCl media to test for complementation. For screening of the X8 library, yeast were transformed with 300 μ g of Kir2.1-RKR-X8 library plasmids, and approximately 2×10^6 clones of transformants (as estimated by growth on 100 mM KCl) were directly plated on 4 mM KCl plates. After 5 days of culture, the rescued colonies were picked and further grown on separate plates for plasmid isolation. To confirm the growth dependence on the plasmid, the isolated plasmids were re-transformed to SGY1528 and tested for growth on 4 mM KCl plates. From approximately 200 clones that were confirmed for the growth upon re-transformation, the X8 sequences were analysed.

Transfection. The HEK293 cells were transiently transfected using FuGENE6 (Roche Applied Sciences, Indianapolis, IN) and were analysed at 24–36 h after transfection.

Flow cytometry. The transfected HEK293 cells were harvested by incubation with 0.5 mM EDTA-PBS for 10 min at 37 °C and washed with Hanks' Balanced Salt Solution supplemented with 5 mM HEPES (pH 7.3) and 2% FBS (staining medium). All the antibody incubations and washings were performed in staining medium at 4 °C. For surface Kir2.1 channel, the cells were stained with rat high-affinity anti-HA monoclonal antibody (Roche) followed by FITC-conjugated goat anti-rat IgG (Vector, Burlingame, CA). For HA-KCNK3 and HA-GPR15, binding of mouse anti-HA antibodies (Santa Cruz Biotechnology, Santa Cruz, CA) was detected by Alexa Fluor 488-conjugated goat anti-mouse IgG (Molecular Probes, Eugene, OR). For surface CD4, FITC-conjugated anti-human CD4 monoclonal antibody (DAKO, Carpinteria, CA) was used. For CD8, mouse anti-human CD8 monoclonal antibody (Santa Cruz Biotechnology) was followed by FITC-conjugated goat anti-mouse IgG. The stained cells were examined for surface expression with FACSCalibur (BD Biosciences, San Jose, CA).

Metabolic labelling. The stable Kir2.1 clones for wild type and RKR-SWTY were cultured overnight, washed with PBS and starved for 1 h at 37 °C in methionine/cysteine-free DMEM supplemented with 5% dialysed FBS. The cells were collected by trypsinization, washed with starve medium and then labelled with 100 μ Ci ml⁻¹ ³⁵S-methionine/cysteine in the tubes for 10 min at 37 °C. After washing five times with ice-cold HBSS, the cells were chased for the times indicated at 37 °C in complete

medium supplemented with 1 mM methionine and cysteine. After chase, the cells were washed with ice-cold HBSS and split into two portions. One half was used to quantify the surface-expressed Kir2.1 proteins by incubating with anti-HA antibody first and then immunoprecipitated with Protein A beads. The other half was directly lysed and precipitated with HA antibody-bound Protein A beads. The eluate samples were resolved on SDS-PAGE, transferred to nitrocellulose and then analysed by autoradiography using a phosphoimaging system (Fujifilm, Stamford, CT)

Immunoprecipitation and immunoblot. For immunoprecipitation, transfected cells were washed with PBS once and lysed with lysis buffer (1% NP40, 25 mM Tris, 150 mM NaCl, pH 7.50) with protease inhibitor cocktails for 20 min at 4 °C. After spinning for 20 min at 11,000g, the supernatant was mixed with Protein A-conjugated agarose beads pre-incubated with 1 μ g of anti-HA antibody or anti-14-3-3 β antibody (Santa Cruz Biotechnology). After a 5-h incubation, the beads were washed five times with lysis buffer and then boiled with 2 \times sample buffer for SDS-PAGE analysis and immunoblot as described⁷. The samples resolved in SDS-PAGE gels were transferred to nitrocellulose and blotted with corresponding primary antibodies followed by HRP-conjugated secondary antibodies. The rabbit polyclonal anti-Kir2.1 antibody was raised against the C-terminal cytoplasmic region corresponding to amino acids 188–428. The immunoblots were developed with the ECL system (Amersham-Pharmacia, Piscataway, NJ).

Affinity precipitation of 14-3-3 by peptides. The biotin-conjugated peptides for SWTY and control sequences were synthesized (Abgent, San Diego, CA) and immobilized on streptavidin-Sepharose beads. The cell lysate of HEK293 was incubated with the peptide-immobilized beads for 5 h and washed five times with lysis buffer. The beads were boiled, and the eluate was analysed for 14-3-3 by SDS-PAGE followed by silver staining.

Immunocytochemistry. HEK293 cells plated on poly-L-lysine-treated coverslips were transiently transfected. The cells were fixed in 4% PFA-PBS for 15 min, and permeabilized in 0.05% Triton X-100-PBS for 5 min, all at room temperature. CD8 was detected with mouse anti-HA antibody (Santa Cruz Biotechnology), followed by Alexa Fluor 488-conjugated goat anti-mouse IgG (Molecular Probes). Coverslips were mounted on glass slides with Vectashield (Vector Labs, Burlingame, CA) and images were captured using confocal microscopy. Spinning Nipkow disc confocal microscopy was performed with an UltraView LCI System (PerkinElmer, Wellesley, MA) in conjunction with an Eclipse 200 inverted microscope (Nikon, Melville, NY). Imaging through a \times 100 oil immersion planar apochromatic lens (numerical aperture 1.4) was accomplished via excitation using the 488 nm line of a Kr/Ar laser.

Selection of native protein C-terminal peptides. For human (*Homo sapiens*), mouse (*Mus musculus*), rat (*Rattus norvegicus*), worm (*Caenorhabditis elegans*) and yeast (*Saccharomyces cerevisiae*), NCBI RefSeq protein databases (curated, non-redundant sets including mRNAs and proteins for known genes and for gene models) were downloaded and searched using a program written in PERL for desired characteristics. Membrane proteins were selected by requiring that the protein names include one of the following keywords: receptor, transporter, transmembrane, membrane, channel, or pore. The other criteria are well described elsewhere in this article. For the Fly (*Drosophila melanogaster*) proteome, proteins that were annotated as plasma-membrane-localized by Flybase (<http://flybase.bio.indiana.edu/annot/fbannquery.hform>) were manually searched for those criteria used with the other organisms (except the membrane keyword criterion).

BIND identifiers. Two BIND identifiers (www.bind.ca) are associated with this manuscript: 319173 and 319174.

Note: Supplementary Information is available on the Nature Cell Biology website.

ACKNOWLEDGMENTS

We thank L. Jan for providing *Kir2.1* and *Kir6.2* cDNAs, S. Goldstein for KCNK3 cDNA, H. Fu for providing 14-3-3 constructs and many insightful discussions, R. Doms for *GPR15* cDNA, M. Spieker and R. Sheng for helping with DNA recovery and sequencing, and the members of the Li laboratory and C. Montell and C. Machamer for helpful comments on this manuscript. We are indebted to S. Goldstein for his invaluable advice on this manuscript. The work is supported by grants from the National Institutes of Health (GM70959 and NS33324 to M.L.); pre-doctoral (to B.C.) and postdoctoral (to H.S.) fellowship awards from the American Heart Association.

COMPETING FINANCIAL INTERESTS

The authors declare that they have no competing financial interests.

Published online at <http://www.nature.com/naturecellbiology/>

Reprints and permissions information is available online at <http://npg.nature.com/reprintsandpermissions/>

- Wallin, E. & von Heijne, G. Genome-wide analysis of integral membrane proteins from eubacterial, archaean, and eukaryotic organisms. *Protein Sci.* **7**, 1029–1038 (1998).
- Bonifacino, J. S. & Glick, B. S. The mechanisms of vesicle budding and fusion. *Cell* **116**, 153–166 (2004).
- Zerangue, N., Schwappach, B., Jan, Y. N. & Jan, L. Y. A new ER trafficking signal regulates the subunit stoichiometry of plasma membrane K(ATP) channels. *Neuron* **22**, 537–548 (1999).
- Viard, P. *et al.* PI3K promotes voltage-dependent calcium channel trafficking to the plasma membrane. *Nature Neurosci.* **7**, 939–946 (2004).
- O'Kelly, I., Butler, M. H., Zilberberg, N. & Goldstein, S. A. Forward transport. 14-3-3 binding overcomes retention in endoplasmic reticulum by dibasic signals. *Cell* **111**, 577–588 (2002).
- Schwappach, B., Zerangue, N., Jan, Y. N. & Jan, L. Y. Molecular basis for K(ATP) assembly: transmembrane interactions mediate association of a K⁺ channel with an ABC transporter. *Neuron* **26**, 155–167 (2000).
- Shikano, S. & Li, M. Membrane receptor trafficking: Evidence of proximal and distal zones conferred by two independent endoplasmic reticulum localization signals. *Proc. Natl Acad. Sci. USA* **100**, 5783–5788 (2003).
- Nishimura, N. & Balch, W. E. A di-acidic signal required for selective export from the endoplasmic reticulum. *Science* **277**, 556–558 (1997).
- Sevier, C. S., Weisz, O. A., Davis, M. & Machamer, C. E. Efficient export of the vesicular stomatitis virus G protein from the endoplasmic reticulum requires a signal in the cytoplasmic tail that includes both tyrosine-based and di-acidic motifs. *Mol. Biol. Cell* **11**, 13–22 (2000).
- Ma, D. *et al.* Role of ER export signals in controlling surface potassium channel numbers. *Science* **291**, 316–319 (2001).
- Nilsson, T., Jackson, M. & Peterson, P. A. Short cytoplasmic sequences serve as retention signals for transmembrane proteins in the endoplasmic reticulum. *Cell* **58**, 707–718 (1989).
- Tang, W. *et al.* Functional expression of a vertebrate inwardly rectifying K⁺ channel in yeast. *Mol. Biol. Cell* **6**, 1231–1240 (1995).
- Chung, J. J., Shikano, S., Hanyu, Y. & Li, M. Functional diversity of protein C-termini: more than zipcoding? *Trends Cell Biol.* **12**, 146–150 (2002).
- Li, M., Unwin, N., Stauffer, K. A., Jan, Y. N. & Jan, L. Y. Images of purified Shaker potassium channels. *Curr. Biol.* **4**, 110–115 (1994).
- Moore, B. & Perez, V. J. *Specific Acidic Proteins of the Nervous System* (ed. Carlson, F. D.) 343–359 (Prentice-Hall, Englewood Cliffs, NJ, 1967).
- Wang, B. *et al.* Isolation of high-affinity peptide antagonists of 14-3-3 proteins by phage display. *Biochemistry* **38**, 12499–12504 (1999).
- Sun, H., Shikano, S., Xiong, Q. & Li, M. Function recovery after chemobleaching (FRAC): evidence for activity silent membrane receptors on cell surface. *Proc. Natl Acad. Sci. USA* **101**, 16964–16969 (2004).
- Fu, H., Subramanian, R. R. & Masters, S. C. 14-3-3 proteins: structure, function, and regulation. *Annu. Rev. Pharmacol. Toxicol.* **40**, 617–647 (2000).
- Yaffe, M. B. How do 14-3-3 proteins work? — Gatekeeper phosphorylation and the molecular anvil hypothesis. *FEBS Lett.* **513**, 53–57 (2002).
- Ganguly, S. *et al.* Melatonin synthesis: 14-3-3-dependent activation and inhibition of arylalkylamine N-acetyltransferase mediated by phosphoserine-205. *Proc. Natl Acad. Sci. USA* **102**, 1222–1227 (2005).
- Lopes, C. M., Gallagher, P. G., Buck, M. E., Butler, M. H. & Goldstein, S. A. Proton block and voltage gating are potassium-dependent in the cardiac leak channel Kcnk3. *J. Biol. Chem.* **275**, 16969–16978 (2000).
- Maresca, M. *et al.* The virotoxin model of HIV-1 enteropathy: involvement of GPR15/Bob and galactosylceramide in the cytopathic effects induced by HIV-1 gp120 in the HT-29-D4 intestinal cell line. *J. Biomed. Sci.* **10**, 156–166 (2003).
- Wade-Evans, A. M., Russell, J., Jenkins, A. & Javan, C. Cloning and sequencing of cynomolgus macaque CCR3, GPR15, and STRL33: potential coreceptors for HIV type 1, HIV type 2, and SIV. *AIDS Res. Hum. Retroviruses* **17**, 371–375 (2001).
- Yuan, H., Michelsen, K. & Schwappach, B. 14-3-3 dimers probe the assembly status of multimeric membrane proteins. *Curr. Biol.* **13**, 638–646 (2003).
- Yaffe, M. B. *et al.* A motif-based profile scanning approach for genome-wide prediction of signaling pathways. *Nature Biotechnol.* **19**, 348–353 (2001).
- Dougherty, M. K. & Morrison, D. K. Unlocking the code of 14-3-3. *J. Cell Sci.* **117**, 1875–1884 (2004).
- Kagan, A., Melman, Y. F., Krummerman, A. & McDonald, T. V. 14-3-3 amplifies and prolongs adrenergic stimulation of HERG K⁺ channel activity. *EMBO J.* **21**, 1889–1898 (2002).
- Mossessova, E., Bickford, L. C. & Goldberg, J. SNARE selectivity of the COPII coat. *Cell* **114**, 483–495 (2003).
- Miller, E. A. *et al.* Multiple cargo binding sites on the COPII subunit Sec24p ensure capture of diverse membrane proteins into transport vesicles. *Cell* **114**, 497–509 (2003).
- Chung, J. J., Yang, H. & Li, M. Genome-wide analyses of carboxyl-terminal sequences. *Mol. Cell. Proteomics* **2**, 173–181 (2003).
- Coblitz, B. *et al.* Carboxyl-terminal recognition by 14-3-3 proteins for surface expression of membrane receptors. *J. Biol. Chem.* (in the press).
- Ma, D. *et al.* Diverse trafficking patterns due to multiple traffic motifs in G protein-activated inwardly rectifying potassium channels from brain and heart. *Neuron* **33**, 715–729 (2002).

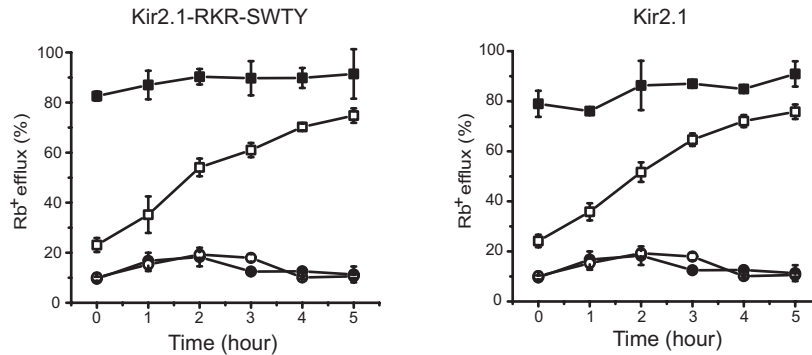


Figure S1 Rate of forward transport as determined by FRAC assay¹⁷. Kir2.1-SWTY and Kir2.1 channels were irreversibly inactivated by [2-(trimethylammonium)ethyl] methanethiosulfonate bromide (MTSET). The recovery of potassium channel activity was measured by Rb⁺ efflux (vertical axis) assayed at 30 °C at the indicated time periods (horizontal axis). 293 cells stably expressing either Kir2.1 (right) or Kir2.1-RKR-SWTY (left) channel after MTSET treatment (open square); Rb⁺ efflux of 293 cells stably

expressing channel proteins without MTSET treatment (filled square) and mock 293 cells treated with (open circle) or without (filled circle) MTSET. This shows that stably expressed Kir2.1 and Kir2.1-SWTY channels both took about 90 minutes to reach 50% recovery ($R_{1/2}$). Hence at both 37 °C¹⁷ and 30 °C, the overall rates of forward transport for Kir2.1 with or without the SWTY motif do not differ significantly.

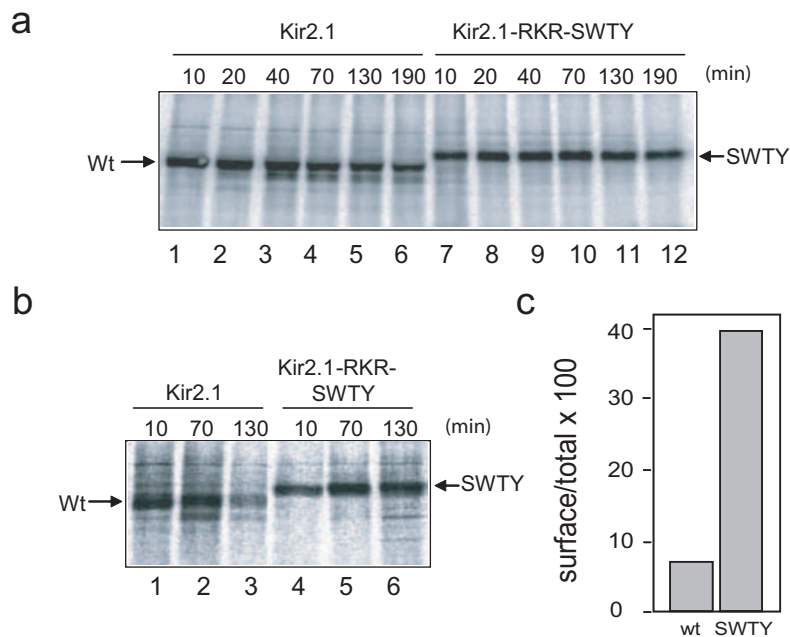


Figure S2 Prolongation of protein half-life on cell surface by SWTY motif. Pulse-chase of Kir2.1 proteins with SWTY motif. a. Wild type Kir2.1 and Kir2.1-RKR-SWTY stable cell lines were pulsed for 10 min at 37 °C, chased at 37 °C for the indicated periods (including pulse time), and then the cell lysates were immunoprecipitated with anti-HA Ab. The overall protein synthesis of two different constructs is similar. b. The pulse-chase studies of the surface fraction of Kir2.1 stable cell lines. The stably transfected cells at different chase periods after pulse were incubated with anti-HA Ab first, lysed, and the Kir2.1 proteins were precipitated by protein A beads. The

wild type (wt) and SWTY-fused Kir2.1 channel peptides are as indicated. The amounts on surface displayed a considerable reduction for Kir2.1 but not for Kir2.1-SWTY, indicating the prolongation of surface half-life by the SWTY motif. c. Quantification of radioactively labeled Kir2.1. The ratios of radioactive signals of surface-immunoprecipitated material vs. total immunoprecipitated material are quantified. The ratios for wt and SWTY at 130 min after pulse are displayed in histograms. The ratio of surface vs. total labeled protein revealed that Kir2.1-SWTY had a more than 4-fold enriched surface partition.